

Universal Magnetic Properties of sp^3 -type Defects in Covalently Functionalized Graphene

Elton J. G. Santos, Andrés Ayuela, Daniel Sánchez-Portal

Centro de Física de Materiales (CFM-MPC), Centro Mixto CSIC-UPV/EHU, Paseo Manuel de Lardizabal 5, 20018 San Sebastián, Spain
Donostia International Physics Center (DIPC), Paseo Manuel de Lardizabal 4, 20018 San Sebastián, Spain

E-mail: elton.jose@gmail.com, swxayfea@ehu.es, sqbsapod@ehu.es

Abstract.

Using density-functional calculations, we study the effect of sp^3 -type defects created by different covalent functionalizations on the electronic and magnetic properties of graphene. We find that the induced magnetic properties are *universal*, in the sense that they are largely independent on the particular adsorbates considered. When a weakly-polar single covalent bond is established with the layer, a local spin-moment of $1.0 \mu_B$ always appears in graphene. This effect is similar to that of H adsorption, which saturates one p_z orbital in the carbon layer. The magnetic couplings between the adsorbates show a strong dependence on the graphene sublattice of chemisorption. Molecules adsorbed at the same sublattice couple ferromagnetically, with an exchange interaction that decays very slowly with distance, while no magnetism is found for adsorbates at opposite sublattices. Similar magnetic properties are obtained if several p_z orbitals are saturated simultaneously by the adsorption of a large molecule. These results might open new routes to engineer the magnetic properties of graphene derivatives by chemical means.

PACS numbers: 73.22.Pr, 73.20.Hb, 75.70.Ak, 75.75.-c

1. Introduction

Graphene has exceptional electronic properties with the potential to give rise to interesting new applications [1, 2, 3]. In particular, graphene is very attractive for spintronics [4]. This is mainly due to the very long spin relaxation and decoherence times in these materials [5, 6]. There have been also numerous claims of the existence of intrinsic magnetism in graphene associated with the presence of structural defects [7, 8, 9, 10, 11, 12, 13], edge states [14, 15], and partial hydrogenation of the layer. [9, 16, 17, 18] These observations suggest that graphene, besides being an ideal material for spintronic circuitry, could also be used in active spintronic devices. An interesting example is provided by graphene nanoribbons. The energies of the polarized states localized at the edges of zigzag nanoribbons or nanotubes can be controlled by external electric fields, and this effect can be used to design a spin-filtering device. [14, 19] However, in spite of the growing interest, to date there has not been a conclusive experimental confirmation of this intrinsic magnetism in graphenic materials. While some experimental groups claim to have found clear indications of ferromagnetism in irradiated graphite [7], graphene prepared from reduced graphene oxide [20] and hydrogenated graphene [21], these results are challenged by other groups with alternative experimental evidences [22, 23].

One of the main difficulties for the observation of ferromagnetism in defective and hydrogenated samples might be related to the bipartite lattice of graphene. It is theoretically well known, at least within a simplified description based on a π -tight-binding Hubbard model, that defects created in different sublattices tend to couple antiferromagnetically [24, 10, 25, 26]. Since, for example, defects created by irradiation are expected to be randomly distributed, this would prevent the formation of ferromagnetic order. Therefore, to generate ferromagnetism in graphene and other graphenic nanostructures, it is desirable to create *all* the defects or to adsorb *all* the hydrogen atoms in *one* of the graphene sublattices. [18] Unfortunately, technically this might be very difficult to achieve. For this reason, it is interesting to look for alternative ways to induce magnetism in the carbon layer. In the present work we analyze, using first-principles electronic structure calculations, the role of different sp^3 -type defects created by covalent functionalization as a source of magnetism in graphene. Covalent functionalization has not been frequently investigated in this context, even though it has been used for a long time in the chemistry of carbon nanostructures and now in graphene [27, 28, 29]. We find that, under very general conditions, any molecule attached to the carbon layer through a weakly-polar single bond produces an effect similar to that of hydrogen adsorption, i.e., induces a significant spin moment in the system. In particular, we explicitly show that the induced magnetism is largely independent on the size of the adsorbed molecule and even on its chemical or biological activity. Regarding the coupling of the induced moments, we show that identical results are obtained by the simultaneous adsorption of several molecules or by the adsorption of a larger molecule that creates several bonds with the layer. This simple fact may open

new and interesting routes to tune the magnetism of graphene. In principle, molecules can be produced with the appropriate structural and chemical characteristics to create bonds with the layer according to predefined patterns. Thus, the powerful techniques of organic and surface chemistry could be applied to synthesize magnetic derivatives of graphene that behave according to well studied theoretical models [24, 10, 25, 26]. This is particularly attractive due to the recent successful syntheses of different graphene derivatives using surface chemical routes [30, 31]. Thus, the synthesis of carbon nanostructures with functional groups at predefined positions, starting from previously functionalized monomers, seems plausible nowadays. Our study deals with the magnetic properties of such nanostructures.

In more detail, our calculations predict that, when a single C–C covalent bond is established between an adsorbate and graphene, a spin moment of $1.0 \mu_B$ is always induced in the system. The size and spatial distributions of these moment are nearly independent of the particular adsorbate. We explicitly show that this effect occurs for a wide class of organic and inorganic molecules with different biological and chemical activity, e.g. alkanes[32], polymers[33, 34, 35], diazonium salts[36, 37, 38], aryl and alkyl radicals[39, 40], nucleobases[41, 42], amide and amine groups[43], glucose,[44] and organic acids[38, 45]. While a similar behavior is observed for hydrogen adsorption, we show for other adsorbates (NH_2 [46], OH [45] and F [47, 48]) that the induced spin-moment decreases with increasing bond-polarity. Moments induced by adsorption in the same sublattice align ferromagnetically, with an exchange coupling that falls off very slowly with the distance between adsorbates ($\sim r^{-(1+\epsilon)}$, $\epsilon \sim 0.20$). In contrast, for molecules adsorbed on opposite sublattices no magnetic solutions could be stabilized.

2. Methods

Our first-principles electronic structure calculations use density functional theory [49] as implemented in the SIESTA code [50]. We use the generalized gradient approximation[51], norm-conserving pseudopotentials[52] and a basis set of numerical atomic orbitals [50]. A double- ζ polarized (DZP) basis set has been used for the calculation of the magnetic moments and electronic band structures of all our systems. We have checked that the relaxed structures with a DZP basis are almost identical to those obtained using a double- ζ (DZ) basis. Therefore, we have used the smaller DZ basis for the relaxations of systems containing more than 100 atoms. The force tolerance for structural optimizations was $0.04 \text{ eV}/\text{\AA}$. The integration over the Brillouin zone was performed using a well converged k -sampling equivalent to $136 \times 136 \times 1$ k -points for the unit cell of graphene. The fineness of the real-space grid used by SIESTA was equivalent to a 150 Ry plane-wave cutoff. We have repeated some calculations with the VASP code[53, 54] using a well-converged plane-wave cutoff energy of 400 eV combined with the projected-augmented-wave (PAW) method. Other computational details were as previously described. The use of PAW potentials allows to check the inherent limitations of the norm-conserving pseudopotentials. The two methods provide

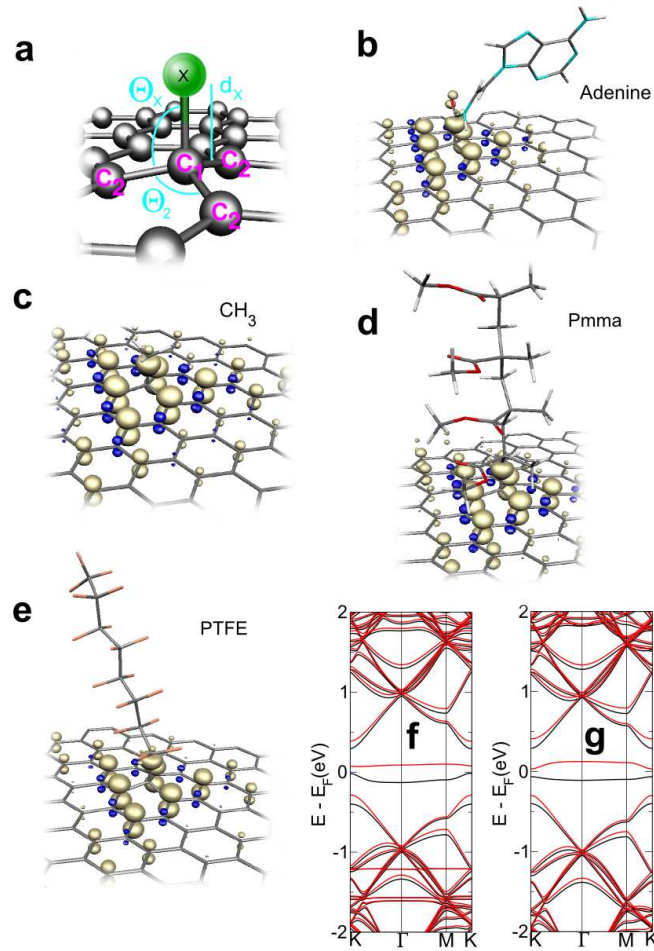


Figure 1. (Color online) (a) Schematic representation of the adsorption geometry of our systems and the nomenclature used in Table 1. X denotes here the atom directly bonded to graphene. Panels (b)-(e) show the isosurfaces ($\pm 0.019 e^-/\text{Bohr}^3$) of the magnetization density induced on graphene by functionalization using adenine derivatives[42], CH_3 , PMMA and PTFE. Majority and minority spin densities correspond respectively to light and dark surfaces, which localize in different graphene sublattices and show a slow decay with distance in all the cases. Panels (f) and (g) show the spin polarized band structures of a 8×8 graphene supercell with a single adenine derivative and a CH_3 molecule chemisorbed on top of one carbon atom, respectively. The black and red (gray) lines denote the majority and minority spin bands, respectively. The Fermi energy is set to zero.

almost identical results. We have checked that, when a sufficiently dense k-sampling is used, our results are very weakly dependent on the supercell size. In particular, a spin moment of $1 \mu_B$ is always associated with the formation of single C-C bonds with graphene, as well as with H adsorption. All the calculations presented in the text used a 8×8 supercell of graphene.

3. Results and discussion

We first calculated the adsorption geometry of several molecules that can establish single bonds with the graphene layer. Most of them are attached to graphene through a single C–C covalent bond (denoted by X=C in Table 1, X being the atom that bonds to graphene). We have also considered other adsorbates (H, NH₂, OH and F) that form heteropolar bonds with graphene. In all cases the adsorbate sits directly on top of one of the C atoms of the layer [see the scheme in Fig. 1 (a)]. This central C atom (C₁) moves vertically and approximately keeps a symmetric three-fold structure respect to its neighbors (C₂). Table 1 describes adsorption geometries of the different molecules. The angles Θ_X and Θ_2 are in the range 102.1° – 107.0° and 111.8° – 115.7° , respectively. These values are half-way between those corresponding to a sp^2 hybridization of the central C₁ atom ($\Theta_X = 90^\circ$ and $\Theta_2 = 120^\circ$), and those expected for a sp^3 local hybridization ($\Theta_X = \Theta_2 = 109.5^\circ$). Thus, the observed geometries can be understood by a slight modification of the sp^2 hybridization of C₁ that gains certain sp^3 character [55]. The largest sp^3 character among the studied molecules corresponds to the adsorption of nitrobenzene (C₆H₄NO₂), anisole (C₆H₄OCH₃), PMMA, and polystyrene groups. The smallest local distortion of the carbon layer corresponds to F adsorption, reflecting a larger ionic character of the interaction.

The main results for the magnetism of all the studied adsorbates are presented in Fig. 1 and Table 1. We first focus on the adsorbates attached to the layer by a single C–C bond. In this case, the graphene-adsorbate complexes always exhibit a spin moment of $1 \mu_B$. The induced spin polarization texture is shown in Fig. 1 for the adsorption of the groups adenine (b) and methyl (c), and the PMMA (d) and PTFE (e) polymers. The calculated patterns are remarkably similar in all the cases. Surprisingly, although the spin moment is induced by the functionalization, it is mostly localized in the graphene layer. The p_z character of the electronic states behind the spin polarization is also evident in the plots. The distribution of the spin moment follows the bipartite character of the graphene lattice: C atoms in the opposite (same) sublattice than the saturated C atom C₁ show majority (minority) spin polarization. Although the total spin moment is $1.0 \mu_B$, a Mulliken analysis only assigns $\sim 0.10 \mu_B$ to the C atoms that form the graphene-adsorbate bond (C₁–X, with X=C). In contrast, the contribution from the three first nearest-neighbors [C₂ in Fig. 1 (a)] is $0.34 \mu_B$, $-0.13 \mu_B$ from the next nearest-neighbors, $0.26 \mu_B$ from the third neighbors, and $0.40 \mu_B$ integrated over larger distances. This clearly shows the slow decay of the spin moment induced in graphene by this type of covalent functionalization. The latter is also reflected in the long-range exchange interactions between adsorbates that we describe below.

In order to understand the origin of this spin polarization we have explored the band structure of the functionalized layers. Figure 1(f) and (g) show the band structure for graphene functionalized with adenine and methyl groups, respectively, as representative cases. The magnetization comes from a very narrow defect state that is pinned at the Fermi level (E_F). This state shows a predominant p_z contribution from the nearest

neighbors C_2 to the defect site, with a much smaller component from the adsorbate itself and a negligible contribution from the central carbon atom C_1 . This state is reminiscent of the defect level that appears associated with a carbon vacancy in a π -tight-binding description of graphene [10]. The origin of the level is also similar in the present case, since the new C–C bond formed upon adsorption saturates the p_z orbital at C_1 . The small dispersion of this p_z -defect band combined with its partially filled character favors the spin-uncompensated solution. Table 1 shows the spin-splitting of the p_z defect-band (δE_s) at Γ point [56]. This splitting varies in the small range 0.19-0.24 eV for all the adsorbates anchored by a single C–C bond (see also Fig. 2). This further confirms the similar character and localization of the defect state behind the spin polarization for all the molecules. The energy gain with respect to the spin-compensated solution ($\Delta E_M = E_{PM} - E_{FM}$) is comparable for all adsorbates, being ~ 45 meV.

The observed spin moment is localized in graphene and, therefore, it is derived from the electronic states of the carbon layer. However, the spin moment appears due to the covalent functionalization with non-magnetic molecules. As mentioned above, the adsorbate saturates the p_z -orbital of one of the C atoms in the layer and, thus, creates a defect analogous to a π -vacancy. Still, according to the results in Table 1, the polarity of the graphene-adsorbate bond is an additional ingredient that determines the size of the spin moment of the system [57]. As the ionic character of the bond increases (going from H to F in Table 1) we observe a transition from a magnetic to a non-magnetic ground state. We can use the results from Mulliken population analyses to characterize the relative polarity of these bonds. Although the absolute values of the charge transfer have to be taken with care, since they are known to be strongly dependent on the size and quality of the basis set, results obtained with the same type of basis set can be compared and used to establish trends [58]. In our calculations both H and NH_2 radicals present almost negligible charge transfers of 0.003 and 0.046 electrons from graphene, respectively. Consequently, H and NH_2 behave similarly to the adsorbates presented previously, i.e., those bonded to graphene through homopolar C–C bonds. The electronic band-structures induced by H and NH_2 are similar to those presented in Fig. 1, and solutions with large spin-moments close to $1 \mu_B$ are also stabilized. In contrast, the charge transfers from graphene to OH and F increase to 0.26 and 0.27 electrons, respectively. As a consequence, the Fermi level and the p_z defect-band pinned to it appear now 0.2-0.3 eV below the Dirac point. This is consistent with the appreciable charge transfer towards the adsorbate and the consequent doping of the layer with holes. The additional population of the defect level, as well as its energy position in a region with a larger density of states of graphene, causes a drastic reduction of the spin moment for OH and a non-magnetic ground state for F. However, calculations using the fixed spin-moment method, presented in parentheses in Table 1, show that the energy penalty needed to develop a spin solution is quite small even in the case of F ($\Delta E_M = -24.1$ meV). Thus, although non-magnetic according to our calculation, the graphene–F bond can be easily polarized (at least in the low adsorbate-density regime explored here). This can be important to interpret the recent experimental report of

Table 1. Results of the structural parameters for all the studied adsorbates. We follow Fig. 1 (a) for the nomenclature. Energy gain ΔE_M due to the spin polarization, total spin moment S and spin-splitting δE_s of the defect level are also included. The numbers in parentheses for F are calculated using the fixed-spin method.

	$d_X(\text{\AA})$	$\Theta_X(^{\circ})$	$\Theta_2(^{\circ})$	$\Delta E_M(\text{meV})$	$S(\mu_B)$	$\delta E_s(\text{eV})$
X = C						
CH ₃	1.59	104.5	113.9	48.6	1.00	0.23
C ₂ H ₅	1.59	105.0	114.0	48.0	1.00	0.23
C ₆ H ₁₁	1.67	105.9	112.5	47.4	1.00	0.23
C ₆ H ₅	1.59	105.7	112.9	46.2	1.00	0.23
C ₆ H ₄ F	1.61	106.6	112.2	45.6	1.00	0.23
C ₆ H ₄ NO ₂	1.60	107.0	111.8	32.3	1.00	0.20
C ₆ H ₄ OCH ₃	1.59	106.9	111.9	38.4	1.00	0.21
C ₆ H ₄ CH ₃	1.61	106.6	112.2	46.6	1.00	0.23
C ₆ H ₄ NH ₂	1.60	106.5	112.3	42.8	1.00	0.22
CONH ₂	1.65	104.9	113.6	43.2	1.00	0.21
COOH	1.60	104.5	113.6	41.6	1.00	0.22
PMMA	1.67	106.8	112.0	47.1	1.00	0.23
PTFE	1.67	105.8	112.9	64.8	1.00	0.19
Adenine derivative*	1.65	104.7	113.8	42.5	1.00	0.23
D-Glucose	1.64	105.1	113.5	41.4	1.00	0.21
Polystyrene	1.60	106.8	112.0	40.0	1.00	0.21
Polyacetylene	1.58	105.0	113.6	50.1	1.00	0.24
X = H, N, O, F						
H	1.12	102.6	115.3	46.5	1.00	0.24
NH ₂	1.52	105.2	113.4	27.7	0.89	0.20
OH	1.52	103.7	114.6	8.4	0.56	0.12
F	1.55	102.1	115.7	0.0	0.00	0.00
				(-24.1)	(1.00)	(0.16)

* 9-(2-aminoethyl)adenine anchored to a carbonyl group [42]

colossal magnetoresistance in this system. [59]

We now look at the electronic structure around E_F in more detail. Fig. 2 shows the calculated density of states (DOS) per spin channel for different adsorbates chemisorbed on graphene through a C–C bond. Despite the curves being shifted and smoothed with a Lorentzian broadening, the data collapse onto a single pattern: one fully polarized peak appears close to E_F . This confirms the universality of the spin moment associated with this type of covalent functionalization, independent of the particular adsorbate. In particular, our results point out to an almost perfect analogy between chemisorbed hydrogen [9, 16, 10] and adsorbates bind to graphene through single C–C bonds, which is not an obvious behaviour. Deviations (not shown in Fig. 2) from this collapsed curve

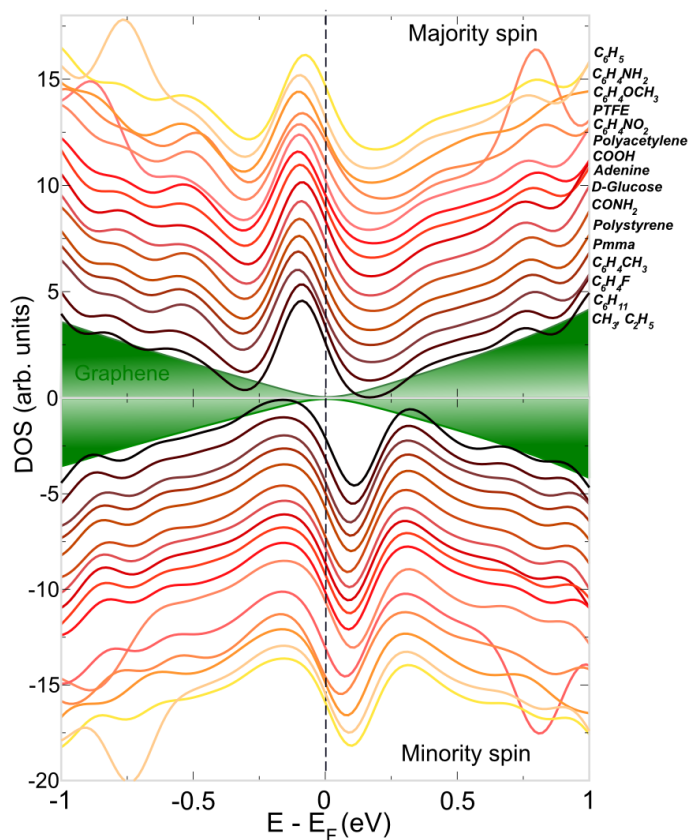


Figure 2. (Color online) Spin-polarized density of states for one molecule chemisorbed on a graphene supercell. All the adsorbates considered attach to the layer through a single C–C bond. For clarity, curves for different adsorbates have been shifted and smoothed with a Lorentzian broadening of 0.12 eV. The Fermi level is marked by the dashed line and is set to zero. The shaded regions denote the density of states of pristine graphene.

are observed for adsorbates that form with graphene bonds of a considerable different character and polarity.

Next we study the magnetic couplings between adsorbates at low concentrations. Figure 3 shows the energy differences between ferromagnetic (FM) and antiferromagnetic (AFM) alignments of the adsorbate-induced spin moments as a function of the distance between the adsorption sites. These results can be used to estimate the size and the distance dependence of the exchange couplings between the adsorbate-induced moments in graphene. We have studied systems of two different kinds: in one case two independent molecules are adsorbed at different locations, while in the other case a single molecule forms two covalent bonds with the graphene layer. To exemplify the first type of system, we have used H and CH_3 as representative adsorbates. Several observations can be made in this case: (i) If the two molecules are located at the same sublattice (AA adsorption), the FM alignment is always more stable than the AFM one. In the FM case, the total spin moment integrates to $2.00 \mu_B$ for both H and CH_3

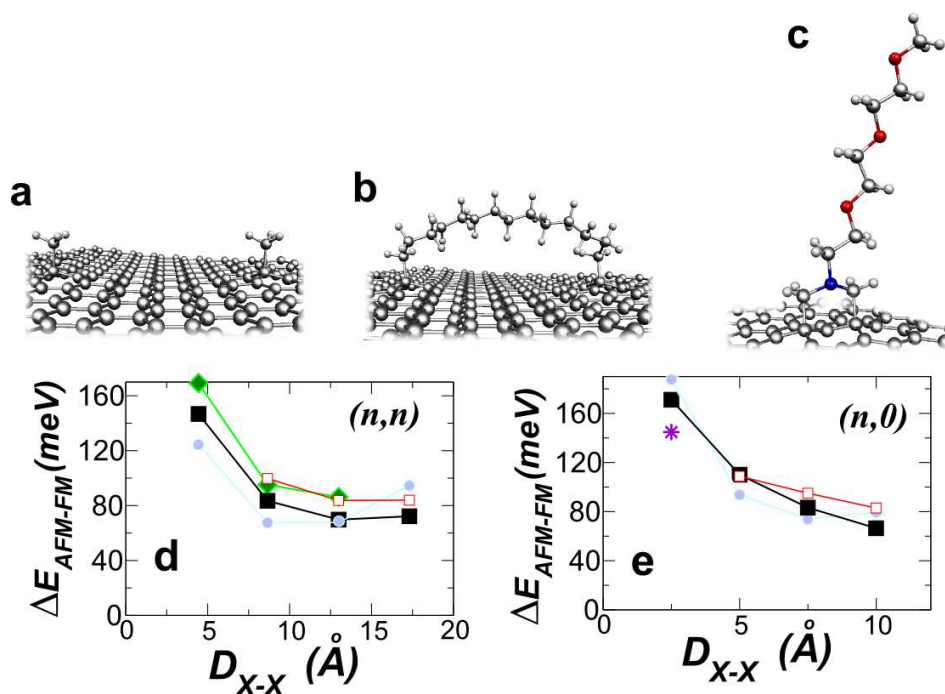


Figure 3. (Color online) Schematic representation of some of the systems used to study the exchange coupling between adsorbate-induced spin moments in graphene: (a) two methyl groups, (b) the two ends of an alkane chain attached at two neighboring locations, and (c) the two bonds formed in a cycloaddition. The calculated energy difference, using a 8×8 supercell, between antiferromagnetic and ferromagnetic alignments of the local spin-moments are shown as a function of the distance along the armchair (d) and zigzag (e) directions. Only data for saturation at the the same graphene sublattice (AA configurations) are shown. Simultaneous adsorption at different sublattices (AB configurations) always gave rise to non-spin-polarized solutions. Filled and empty squares correspond, respectively, to H and CH₃. Diamonds (green symbols) in panel (d) stand for the alkane chain and the star in panel (e) for the hypothetical AA-cycloaddition shown in (c). Circles (gray symbols) correspond to the best fit using a Heisenberg model (see text).

and the local spin population remains nearly constant around each defect site, roughly insensitive to the presence of the neighboring adsorbate; (ii) If the two molecules are at the different sublattices (AB adsorption), we could not stabilize any magnetic solution, and the system converges to a spin-compensated solution with no local moment; (iii) The size and distance dependence of the magnetic couplings are very similar for H and CH₃, which further supports the analogy presented above; (iv) For two methyl groups at short distances (< 5.0 Å) we could only find FM solutions.

We have also considered the magnetic couplings between local spin-moments induced in the layer by the formation of two single C–C bonds between graphene and the *same* molecule. We first explore this situation using a long alkane chain attached to graphene at two different locations [see Fig. 3 (b)]. Since the characteristics of the spin moment induced by covalent functionalization are quite independent of the adsorbed

molecules, as far as they are anchored by a single C-C bond, we expect in this case a result similar to that previously found for two methyl groups. This is confirmed by the results in Fig. 3 (d). For AA adsorption, i.e., when the two bonds between the alkane chain and graphene are established with atoms in the same graphene sublattice, the FM alignment with a $2 \mu_B$ total spin moment is still the most stable. The size of the exchange couplings is almost identical to the case of two independent methyl groups. The only significant difference is that for the alkane chain we succeeded to find an AFM configuration at short distances. Furthermore, in the present case AB adsorption also converges to spin-compensated solutions.

Figure 3 (c) and (e) show another example of magnetism associated with several bonds formed by the same molecule. In this case, we have considered a dipolar cycloaddition [60, 61]. Usually this kind of cycloaddition saturates simultaneously two first-neighbor carbon atoms in graphene, i.e., it corresponds to an AB configuration. As a consequence, in agreement with the results presented so far, the cycloaddition does not create a spin moment in the layer. However, we have considered here another configuration in which the molecule is attached to two second-neighbor carbon atoms in graphene. This artificial AA-cycloaddition is 1.18 eV less stable than the standard AB-cycloaddition. In accordance to the universality of our results so far, the AA-cycloaddition gives rise to a spin-polarized solution. As expected, the FM solution with $2\mu_B$ spin moment is more stable, and the estimated exchange coupling fits well with those found for H, the methyl radical and the alkane chains.

The observed magnetic behavior follows closely the expectations based on Lieb's theorem for a bipartite Hubbard model at half-filling [24], which is an appropriate model to describe the low energy electronic excitations in graphene. Lieb's theorem predicts that graphene should develop a *total* spin moment of $2\mu_B$ for AA adsorption and zero for AB adsorption [24, 10]. However, this does not explain why a spin-compensated solution is more stable than an AFM solution for AB adsorption, as we find in our first-principles calculations. The reason for this behavior can be rationalized as follows. When adsorption takes place at opposite sublattices, due to the bipartite character of graphene, the interaction between defect levels in neighboring adsorption sites is appreciable. This interaction opens a bonding-antibonding gap in the p_z -defect bands that contributes to stabilize the spin-compensated solution. The non-magnetic solution is favored when this gap is larger than the spin splitting δE_s of the isolated defect [62]. A detailed analysis of the calculated band structures confirms this interpretation. It is noteworthy that a similar behavior was also observed for chemisorbed hydrogen [9, 16], vacancies [63, 10], and even for substitutional Co atoms in graphene [62]. All of them exhibit a very similar electronic structure nearby E_F . According to our interpretation, at sufficiently large distances between the adsorbates, a magnetic configuration with non-zero local spin-moments at each adsorption site should become favorable even for AB adsorption. At such long distances, the gap in the defect band becomes smaller than δE_s and the local spin-moments are recovered. However, in accordance with Lieb's theorem, an AFM configuration will be favored in this case. The necessary distances to

stabilize these AFM solutions are larger than those explicitly considered in our *ab initio* calculations presented in Fig. 3. The co-existence of non-magnetic and AFM solutions for AB configurations has been observed using first-principles calculations in the case of substitutional Co atoms in graphene [62].

An important consequence of the results presented above is that it is possible to turn graphene magnetic by chemical functionalization [21]. Unfortunately, they also tell us that, in order to achieve and control such magnetism, it is necessary to have selectivity on the adsorption site, i.e., molecules should preferentially attach to one of the graphene sublattices. This can be difficult to achieve in practice, particularly if we take into account that AA configurations are usually less favorable than AB configurations [16, 17]. Therefore, some difference must be introduced between A and B sites to promote adsorption on a single sublattice. For example, one possibility could be the registry with an appropriate substrate, but this can also alter other desired properties of the graphene layer. Fortunately, our results also show that it is not necessary to adsorb several molecules to obtain large spin moments in graphene. A similar effect is obtained by adsorbing a *single* molecule that simultaneously establishes several C–C covalent bonds with the layer. This simple observation might open a new route to engineer the magnetism of graphene derivatives. In principle, *molecules could be synthesized with the appropriate distances between anchoring groups* so, when adsorbed on graphene, all bonds will be formed with atoms in the same graphene sublattice. The spin moment associated with the adsorption of such molecules would be equal to the number of C–C bonds with graphene. Furthermore, the stability of this spin moment will be enhanced due to the strong FM interactions between nearby localized moments in the same sublattice.

We have also analyzed our results for the magnetic interactions within the framework of a classical Heisenberg model. The interactions are described by the model Hamiltonian $H = \sum_{i<j} J(\mathbf{r}_{ij}) \mathbf{S}_i \mathbf{S}_j$, where $J(\mathbf{r}_{ij})$ is the exchange constant and \mathbf{S}_i is the local moment induced by covalent functionalization. The expression for the angular dependence of the exchange has been taken from the RKKY-like coupling obtained analytically in Ref. [64]. A simple $|r_{ij}|^\alpha$ behavior was assumed for the distance dependence, and the exponent α was fitted to our *ab initio* results in the case of AA-adsorption. We find that the interaction between the chemisorbed molecules in graphene surface is long range and falls off slowly with the distance, roughly proportional to $J_{AA}(\mathbf{r}_{ij}) \sim |r_{ij}|^{-(1+\epsilon)}$ with $\epsilon \sim 0.20$. [see the circles in Fig. 3 (d) and (e)]. This distance decay agrees well with a recent theoretical study using a π -tight-binding model [65], where the interaction between adatoms on graphene was shown to decay as the inverse of the distance. In contrast, exchange interactions between substitutional Co impurities in graphene, a system that in principle can also be assimilated to a π -vacancy or H adsorption, were recently shown to decay much faster ($\sim |r_{ij}|^{-2.43}$) [62]. This is probably related to the larger localization of the spin moment in the latter case, associated with the 3d Co contribution.

4. Conclusions

We have shown that covalent functionalization can be used to switch on the magnetism of graphene. Notwithstanding its structure and chemical or biological activity, when a molecule chemisorbs on graphene with the formation of a single C–C covalent bond between the adsorbate and the layer, a spin moment of $1.0 \mu_B$ is always induced in the system. This universal spin moment is almost exclusively localized in graphene, and its origin can be traced back to the polarization of a defect state that appears nearby the Fermi level. A similar effect accompanies the functionalization of carbon nanotubes [66], and the chemisorption of hydrogen on graphene. This behavior is also reminiscent of the polarization observed for a single vacancy in a π -tight-binding description of the carbon monolayer. Other types of bonding, mediated by species different from C, also show similar magnetic properties as far as the established bond is not strongly polar. If chemisorption is accompanied by a substantial charge transfer between the adsorbate and graphene, the spin polarization is reduced and eventually disappears, as it is the case of F adsorption. However, even in this case, the low energy cost necessary to polarize the system seems to indicate that the magnetic properties of fluorinated graphene can be tuned using moderate magnetic fields. [59]

Similar to the moment formation, exchange interactions are also found to be very weakly dependent on the nature of the adsorbates. In particular, we have explicitly checked that hydrogen atoms and methyl radicals give rise to the same magnetic couplings. Adsorbates in the same graphene sublattice (AA adsorption) couple ferromagnetically with an exchange interaction that decays almost inversely proportional to the distance $J_{AA}(\mathbf{r}_{ij}) \sim |r_{ij}|^{-(1+\epsilon)}$ with $\epsilon \sim 0.20$. In contrast, the larger effective electronic hoppings between adsorbates at different sublattices (AB adsorption) prevent magnetism from arising in that situation. We have checked that the same results are obtained irrespective of whether the C–C bonds are established by the simultaneous adsorption of several molecules or by the adsorption of a single larger molecule. Therefore, the observed behavior is intrinsic to graphene and appears associated with the saturation of a given collection of p_z orbitals in the layer. This might open new routes to engineer the magnetism of graphene derivatives since, in principle, molecules can be produced with the appropriate structural and chemical characteristics to simultaneously bond to several atoms in the same graphene sublattice. The spin moment arising from such an adsorption will be proportional to the number of covalent bonds established and will have an enhanced stability due to the ferromagnetic interactions between nearby saturations in the same sublattice. Our findings are particularly attractive in the light of the recent successful synthesis of different graphene derivatives using surface chemical routes [30, 31]. Therefore, the synthesis of carbon nanostructures with functional groups at predefined positions, starting from previously functionalized monomers, seems plausible nowadays.

Acknowledgments

We acknowledge support from Basque Departamento de Educación and the UPV/EHU (Grant No. IT-366-07), the Spanish Ministerio de Educación y Ciencia (Grant No. FIS2010-19609-CO2-02) and the ETORTEK program funded by the Basque Departamento de Industria and the Diputación Foral de Gipuzkoa. DSP wants to acknowledge useful discussions with Dr. G. Teobaldi.

References

- [1] Geim A K and Novoselov K S 2007 *Nature Materials* **6** 183–191
- [2] Castro Neto A H, Guinea F, Peres N M R, Novoselov K S and Geim A K 2009 *Rev. Mod. Phys.* **81** 109–162
- [3] Geim A K 2009 *Science* **324** 1530–1534
- [4] Wolf S A, Awschalom D D, Buhrman R A, Daughton J M, Molnar S V, Roukes M L, Chtchelkanova A Y and Treger D M 2001 *Science* **294** 1488–1495
- [5] Hueso L E, Pruneda J M, Ferrari V, Burnell G, Valdés-Herrera J P, Simons B D, Littlewood P B, Artacho E, Fert A and Mathur N D 2007 *Nature* **445** 410–413
- [6] Trauzettel B, Bulaev D V, Loss D and Burkard G 2007 *Nature Phys.* **3** 192–196
- [7] Esquinazi P, Spemann D, Höhne R, Setzer A, Han K H and Butz T 2003 *Phys. Rev. Lett.* **91** 227201
- [8] Lehtinen P O, Foster A S, Ayuela A, Krasheninnikov A V, Nordlund K and Nieminen R 2003 *Phys. Rev. Lett.* **91** 017202
- [9] Yazyev O V and Helm L 2007 *Phys. Rev. B* **75** 125408
- [10] Palacios J J, Fernández-Rossier J and Brey L 2008 *Phys. Rev. B* **77** 195428
- [11] Ugeda M M, Brihuega I, Guinea F and Gómez-Rodríguez J M 2010 *Phys. Rev. Lett.* **104** 096804
- [12] Yazyev O V 2010 *Rep. Prog. Phys.* **73** 056501
- [13] Banhart F, Kotakoski J and Krasheninnikov A 2011 *ACS Nano* **5** 26–41
- [14] Son Y W, Cohen M L and Louie S G 2006 *Nature* **444** 347–351
- [15] Yazyev O V and Katsnelson M I 2008 *Phys. Rev. Lett.* **100** 047209
- [16] Boukhvalov D W, Katsnelson M I and Lichtenstein A I 2008 *Phys. Rev. B* **77** 035427
- [17] Casolo S, Lovvik O M, Martinazzo R and Tantardini G F 2009 *J. Chem. Phys.* **130** 054704
- [18] Zhou J, Wang Q, Sun Q, Chen X S, Kawazoe Y and Jena P 2009 *Nano Lett.* **9** 3867–3870
- [19] Mañanes A, Duque F, Ayuela A, López M J and Alonso J A 2008 *Phys. Rev. B* 035432
- [20] Wang Y, Huang Y, YSong, Ma X Z Y, Liang J and Chen Y 2009 *Nano Lett.* **8** 220–224
- [21] Xie L, Wang X, Lu J, Ni Z, Luo Z, Mao H, Wang R, Wang Y, Huang H, Qi D, Liu R, Yu T, Shen Z, Wu T, Peng H, Özyilmaz B, Loh K, Wee A T S, Ariando and Chen W 2011 *Appl. Phys. Lett.* **98** 193113
- [22] Sepioni M, Nair R R, Rablen S, Narayanan J, Tuna F, Winpenny R, Geim A K and Grigorieva I V 2010 *Phys. Rev. Lett.* **105** 207205
- [23] Martínez-Martín D, Jaafar M, Pérez R, Gómez-Herrero J and Asenjo A 2010 *Phys. Rev. Lett.* **105** 257203
- [24] Lieb E H 1989 *Phys. Rev. Lett.* **62** 1201
- [25] Soriano D, Leconte N, Ordejón P, Charlier J C, Palacios J J and Roche S 2011 *Phys. Rev. Lett.* **107** 016602
- [26] Leconte N, Soriano D, Roche S, Ordejón P, Charlier J C and Palacios J J 2011 *ACS Nano* **5** 3987–3992
- [27] Hirsch A 2002 *Angew. Chem. Int. Ed.* **41** 1853–1859
- [28] Park S and Ruoff R S 2009 *Nature Nanotech.* **4** 217–224
- [29] Loh K P, Bao Q, Ang P K and Yang J 2010 *J. Mater. Chem.* **20** 2277–2289

- [30] Cai J, Ruffieux P, Jaafar R, Bieri M, Braun T, Blakenburg S, Muoth M, Seitsonen A P, Saleh M, Feng X, Müllen K and Fasel R 2010 *Nature* **466** 470–473
- [31] Treier M, Pignedoli C A, Laino T, Rieger R, Müllen K, Passerone D and Fasel R 2010 *Nature Chemistry* **3** 61–67
- [32] Meyer J C, Girit C O, Crommie M F and Zettl A 2008 *Nature* **454** 319–322
- [33] Ramanathan T, Abdala A A, Stankovich S, Dikin D A, Herrera-Alonso M, Piner R D, Adamson D H, Schniepp H C, Chen X, Ruoff R S, Nguyen S T, Aksay I A, Homme R K P and Brinson L C 2008 *Nature Nanotech.* **3** 327–331
- [34] Fang M, Wang K, Lu H, Yang Y and Nutt S 2009 *J. Mater. Chem.* **19** 7098–7105
- [35] Liu N, Luo F, Wu H, Liu Y, Zhang C and Chen J 2008 *Adv. Funct. Mater.* **18** 1518–1525
- [36] Sinitskii A, Dimie A, Corle D A, Fursin A A, Kosynkin D V and Tour J M 2010 *ACS Nano* **4** 1949–1954
- [37] Zhu Y, Higginbotham A L and Tour J M 2009 *Chem. Mater.* **21** 5284–5291
- [38] Lomeda J R, Doyle C D, Kosynkin D V, Hwang W F and Tour J M 2008 *J. Am. Chem. Soc.* **130** 16201–16206
- [39] Niyogi S, Bekyarova E, Itkis M E, Zhang H, Shepperd K, Hicks J, Sprinkle M, Berger C, Lau C N, deHeer W A, Conrad E H and Haddon R C 2010 *Nano Lett.* **10** 4061–4066
- [40] Cao Y, Feng J and Peiyi W 2010 *Carbon* **48** 1683–1685
- [41] Varghese N, Mogera U, Govindaraj A, Das A, Maiti P K, Sood A K and Rao C N R 2009 *ChemPhysChem* **10** 206–210
- [42] Singh P, Kumar J, Toma F M, Raya J, Prato M, Fabre B, Verma S and Bianco A 2009 *J. Am. Chem. Soc.* **131** 13555–13562
- [43] Hsiao M C, Liao S H, Yen M Y, Liu P I, Pu N W, Wang C A and Ma C C M 2010 *ACS Appl. Mater. Interfaces* **2** 3092–3099
- [44] Saha A, Basiruddin S, Ray S C, Roy S S and Jana N R 2010 *Nanoscale* **2** 2777–2782
- [45] Stankovich S, Dikin D A, Piner R D, Kohlhaas K A, Kleinhammes A, Yuanyuan J, Wu Y, Nguyen S T and Ruoff R S 2007 *Carbon* **45** 1558–1565
- [46] Lai L, Chen L, Zhan D, Sun L, Liu J, Lim S H, Poh C K, Shen Z and Lin J 2011 *Carbon* **49** 3250–3257
- [47] Nair R R, Ren W, Jalil R, Riaz I, Kravets V G, Britnell L, Blake P, Schedin F, Mayorov A S, Yuan S, Katsnelson M I, Cheng H M, Strupinski W, Bulusheva L G, Okotrub A V, Grigorieva I V, Grigorenko A N, Novoselov K S and Geim A K 2010 *Small* **6** 2877–2884
- [48] Hong X, Cheng S H, Herding C and Zhu J 2011 *Phys. Rev. B* **83** 085410
- [49] Kohn W and Sham L J 1965 *Phys. Rev.* **140** A1133–A1138
- [50] Soler J M, Artacho E, Gale J D, García A, Junquera J, Ordejón P and Sánchez-Portal D 2002 *J. Phys.: Condensed Matter* **14** 2745–2779
- [51] Perdew J P, Burke K and Ernzerhof M 1996 *Phys. Rev. Lett.* **77** 3865–3868
- [52] Troullier N and Martins J L 1991 *Phys. Rev. B* **43** 1993–2006
- [53] Kresse G and Hafner J 1993 *Phys. Rev. B* **47** 558–561
- [54] Kresse G and Furthmüller J 1996 *Phys. Rev. B* **54** 11169–11186
- [55] Wehling T O, Katsnelson M I and Lichtenstein A I 2009 *Phys. Rev. B* **80** 085428
- [56] We can see in Fig. 1(f)-(g) that other bands also suffer a splitting due to the spin polarization induced by the defect. However, those splittings are much smaller than that of the p_z defect-state close to E_F
- [57] We have also confirmed the key role of the electronegativity of the adsorbate in determining the magnetic properties of covalently functionalized graphene using models based on a simple π -tight-binding description of graphene supplemented with a Hubbard term.
- [58] Sánchez-Portal D, Artacho E and Soler J M 1996 *J. Phys.: Condens. Matter* **8** 3859–3880
- [59] Hong X, Cheng S H, Herding C and Zhu J 2010 *Phys. Rev. B* **83** 085410
- [60] Quintana M, Spyrou K, Grzelczak M, Browne W R, Rudolf P and Prato M 2010 *ACS Nano* **4** 3527–3533

- [61] Cao Y and Houk K N 2011 *J. Mater. Chem.* **21** 1503–1508
- [62] Santos E J G, Sánchez-Portal D and Ayuela A 2010 *Phys. Rev. B* **81** 125433
- [63] Kumazaki H and Hirashima D S 2007 *J. Phys. Soc. Jpn.* **76** 064713
- [64] Saremi S 2007 *Phys. Rev. B* **76** 184430
- [65] Shytov A V, Abanin D A and Levitov L S 2009 *Phys. Rev. Lett.* **103** 016806
- [66] Santos E J G, Sánchez-Portal D and Ayuela A 2011 *Appl. Phys. Lett.* **99** 062503